

NUMERICAL STUDY OF THE AMICK-SCHONBEK SYSTEM

CHRISTIAN KLEIN AND JEAN-CLAUDE SAUT

In memoriam Vassilios Dougalis (1949-2022)

ABSTRACT. The aim of this paper is to present a survey and a detailed numerical study on a remarkable Boussinesq system describing weakly nonlinear, long surface water waves. In the one-dimensional case, this system can be viewed as a dispersive perturbation of the hyperbolic Saint-Venant (shallow water) system. The asymptotic stability of the solitary waves is numerically established. Blow-up of solutions for initial data not satisfying the non-cavitation condition as well as the appearance of dispersive shock waves are studied.

1. INTRODUCTION

Our friend Vassilios Dougalis wrote more than ten papers on the theory and numerical simulations of a class of long water wave systems, and we will focus in this paper on one specific member of this class.

More precisely we will consider a particular case of the so-called abcd Boussinesq systems for surface water waves, see [8, 9, 10]¹

$$(1.1) \quad \begin{cases} \eta_t + \nabla \cdot \mathbf{v} + \epsilon \nabla \cdot (\eta \mathbf{v}) + \mu [a \nabla \cdot \Delta \mathbf{v} - b \Delta \eta_t] = 0 \\ \mathbf{v}_t + \nabla \eta + \epsilon \frac{1}{2} \nabla |\mathbf{v}|^2 + \mu [c \nabla \Delta \eta - d \Delta \mathbf{v}_t] = 0. \end{cases}$$

Here $\eta = \eta(x, t)$, $x \in \mathbb{R}^d$, $d = 1, 2$, $t \in \mathbb{R}$ is the elevation of the wave, $\mathbf{v} = \mathbf{v}(x, t)$ is a measure of the horizontal velocity, μ and ϵ are the small parameters (shallowness and nonlinearity parameters respectively) defined as

$$\mu = \frac{h^2}{\lambda^2}, \quad \epsilon = \frac{\alpha}{h}$$

where α is a typical amplitude of the wave, h a typical depth and λ a typical horizontal wavelength.

In the Boussinesq regime, ϵ and μ are supposed to be small and of same order, $\epsilon \sim \mu \ll 1$, and we will take for simplicity $\epsilon = \mu$, writing (1.1) as²

$$(1.2) \quad \begin{cases} \eta_t + \nabla \cdot \mathbf{v} + \epsilon [\nabla \cdot (\eta \mathbf{v}) + a \nabla \cdot \Delta \mathbf{v} - b \Delta \eta_t] = 0 \\ \mathbf{v}_t + \nabla \eta + \epsilon [\frac{1}{2} \nabla |\mathbf{v}|^2 + c \nabla \Delta \eta - d \Delta \mathbf{v}_t] = 0. \end{cases}$$

The coefficients (a, b, c, d) are restricted by the condition

$$a + b + c + d = \frac{1}{3} - \tau,$$

where $\tau \geq 0$ is the surface tension coefficient.

Date: March 20, 2024.

¹Boussinesq [11] was the first to derive particular Boussinesq systems, not in the class of those studied here though. We refer to [16, 17, 18] for details and for an excellent history of hydrodynamics in the nineteenth century.

²Particular cases are formally derived in [12, 19, 34].

When restricted to one-dimensional, unidirectional motions, (1.2) leads to the Korteweg-de Vries (KdV) equation, see [30] (section 9.3)

$$u_t + u_x + \epsilon \left(\frac{1}{3} - \tau \right) u_{xxx} + \epsilon u u_x = 0.$$

The class of systems (1.1), (1.2) models water waves on a flat bottom propagating in both directions in the aforementioned regime (see [8, 9, 10]).

All (well-posed) members of the abcd class provide the same approximation of the water wave system in the Boussinesq regime, with an error of order $O(\epsilon^2 t)$ (see [8]), and their dispersion relations are similar in the long wave regime. Nevertheless they possess quite different mathematical properties as nonlinear dispersive systems due to the very different behavior of the dispersion relation at high frequencies. Actually the order of their dispersive part can vary from +3 to -1, [9, 10]. This makes their mathematical study quite fascinating.

It turns out that two particular one-dimensional cases of the abcd systems have remarkable properties. We focus here on one of them ³ that we will refer to as the *Amick-Schonbek system* ⁴ corresponding to $a = b = c = 0, d > 0$, say $d = 1$ writing thus

$$(1.3) \quad \begin{cases} \eta_t + v_x + \epsilon(\eta v)_x = 0 \\ v_t + \eta_x + \epsilon(vv_x - v_{xxt}) = 0. \end{cases}$$

It appears to be the BBM regularization of the (linearly ill-posed) system

$$(1.4) \quad \begin{cases} \eta_t + v_x + \epsilon(\eta v)_x = 0 \\ v_t + \eta_x + \epsilon(vv_x + \eta_{xxx}) = 0, \end{cases}$$

which is obtained from the Zakharov-Craig-Sulem formulation of the water wave system after expanding the Dirichlet-to-Neumann operator at first order in ϵ . From now on we will take $\epsilon = 1$.

There have been many papers dealing with the numerical study of the Amick-Schonbek system, see for instance [3, 4]. The case of a non-flat bottom is considered in [24] and the periodic case in [5]. Solitary waves were constructed in [14], where their interaction was also studied.

As aforementioned the Amick-Schonbek is the only member of the (one-dimensional) abcd systems for which the global well-posedness of the Cauchy problem with arbitrary large initial data is known. The asymptotics in large time of these solutions is not established, and the simulations in this paper will give some insight into this issue. We will consider in particular the possible soliton decomposition. To this end we study the 1D case with a Fourier spectral method similar to the one for the Serre-Green-Naghdi equation in [20] and get, see also [14, 3], the following

Conjecture I:

The solitary waves of the Amick-Schonbeck system are asymptotically stable. The

³The other one, referred to as the Kaup-Broer-Kupperschmidt system will be considered in a subsequent paper.

⁴Actually this system is a particular case of a system derived by Peregrine in [34], and it is often referred to as the Peregrine or classical Boussinesq system, but Schonbek and Amick were the first to recognize its remarkable mathematical properties. A variant with slowly varying bottom is derived in [39, 40].

long time behavior of solutions to this system for Schwartz class initial data is given by solitary waves plus radiation.

In addition we study the behavior of solutions when the initial data η_0 do not satisfy the non-cavitation condition. We get

Conjecture II:

Solutions to initial data not satisfying the non-cavitation condition $1 + \eta(x, 0) > 0$ can blow up in finite time.

We also address the zero dispersion limit of the AS system in the form (7.1) including the formation of dispersive shock waves (DSWs), zones of rapid modulated oscillations. We conjecture that such DSWs can be observed in the vicinity of shocks of the corresponding dispersionless equation, the Saint Venant system (7.2), for the same initial data. There will not be a strong limit of these DSWs in the limit $\epsilon \rightarrow 0$ in (7.1) as in the case of dissipative equations as the Burgers' equation.

This paper is organized as follows. In section 2 we review the known theoretical results and open problems on the Cauchy problem for the Amick-Schonbek system. In section 3 we numerically construct solitary waves. Perturbations of these solitary waves are studied in section 4. In section 5 we address the long time behavior of hump-like initial data from the Schwartz class. In section 6 we consider initial data not satisfying the non-cavitation condition. Dispersive shock waves are studied in section 7. We add some concluding remarks in section 8.

2. THE CAUCHY PROBLEM

In this section, we collect some known facts on the Amick-Schonbek systems.

As first noticed in a pioneering work by Schonbek [37], the Amick-Schonbek system is among the family of abcd systems the only one that can be viewed as a dispersive perturbation of the Saint-Venant (shallow water) system in the sense that it captures some features of the hyperbolic character of the Saint-Venant system.

Actually Schonbek [37] used a parabolic regularization of the first equation in (1.3), to derive from the entropy of the Saint-Venant system an estimate leading to the global well-posedness of the Cauchy problem for arbitrary large smooth, compactly supported initial data. Amick [2] weakened the required regularity of the initial data and proved uniqueness. Roughly speaking, under a non-cavitation condition that ensures that the underlying Saint-Venant system is hyperbolic, the *positive convex entropy* of the Saint-Venant system implies an a priori global bound on the solutions of (1.3) leading to the global existence and uniqueness of solutions without size restrictions.

The Cauchy problem was recently revisited in [33] where the following result is obtained:

Theorem 2.1. *Let $s > 1/2$. For $(\zeta, u_0) \in H^s(\mathbb{R}) \times H^{s+1}(\mathbb{R})$ such that $1 + \zeta_0 > 0$, the Boussinesq system (1.3) has a solution $(\zeta, u) \in C(\mathbb{R}_+, H^s(\mathbb{R}) \times H^{s+1}(\mathbb{R})) \cap C^1(\mathbb{R}_+, H^{s-1}(\mathbb{R}) \times H^s(\mathbb{R}))$. This solution satisfies $1 + \zeta(t, x) > 0$ for any $t \geq 0$, and is the unique solution of (1.3) that belongs to $L_{loc}^\infty(\mathbb{R}_+; H^s(\mathbb{R}) \times H^{s+1}(\mathbb{R}))$.*

For any $T > 0$, the flow-map $S : (\zeta_0, u_0) \rightarrow (\zeta, u)$ is continuous from $H^s(\mathbb{R}) \times H^{s+1}(\mathbb{R})$ into $C([0, T]; H^s(\mathbb{R}) \times H^{s+1}(\mathbb{R}))$.

As a consequence, Molinet *et al* derived the existence of a global weak solution $(\zeta, u) \in L^\infty(\mathbb{R}^+; \Lambda_{\sigma_0} \times H^1)$ of the Amick-Schonbek system where Λ_{σ_0} is the Orlicz class associated to the entropy:

$$\Lambda_{\sigma_0} = \left\{ \eta \text{ measurable} \mid \int_{\mathbb{R}} (\eta \ln \eta - \eta + 1) dx < +\infty \right\}.$$

These results exploit the hyperbolic nature of the underlying Saint-Venant system. We do not know of similar results in the two-dimensional case (the "long time" existence of solutions to the Cauchy problem was established in [36, 13]).

Remark 2.1. It is very unlikely that the previous global results persist when the non-cavitation condition is not satisfied by the initial data ζ_0 . Then the Cauchy problem remains of course locally well-posed, but a finite time blow-up (of which kind?) might occur.

Remark 2.2. The asymptotic behavior of global solutions provided by the previous theorem is unknown. In particular the possible growth in time of the $H^s \times H^{s+1}$ -norm of (ζ, u) and a lower bound on $(1 + \zeta)$ are interesting open issues. The numerical simulations below suggest a soliton resolution property that would imply the boundedness of the L^∞ norms of solutions. No positive lower bound of the infimum of $1 + \zeta$ was observed.

Remark 2.3. A derivation of $L^1 - L^\infty$ estimates for the linearization at the trivial solution of a large subclass of (abcd) systems, involving the Amick-Schonbek system in spatial dimensions one and two, is provided in [31] together with the corresponding Strichartz and Morawetz estimates.

Remark 2.4. The Amick-Schonbek system possesses for any $C > 1$ unique solitary wave solutions $V(x - Ct), Q(x - Ct)$ such that $V = V(\xi)$, $\xi = x - Ct$, is even, monotonically decreasing when $\xi > 0$, see [14] and section 3 below for details. As far as we know the stability properties of those solitary waves are unknown, and the numerics in section 4 will give some insight into this issue and into their possible role in the long time dynamics of solutions.

Remark 2.5. A viscous regularization of the Amick-Schonbek system different from the one used in [2, 37, 33] is proposed in [7], namely

$$(2.1) \quad \begin{cases} \zeta_t + u_x + (\zeta u)_x = 0 \\ u_t + \zeta_x + uu_x - u_{xxt} - \nu u_{xx} = 0, \end{cases}$$

for which the existence and uniqueness (up to translations) of traveling wave solutions with non zero limit at $-\infty$ is established. They are categorized into dispersive or regularized shock waves depending on the balance between the dispersive and dissipative effects.

Remark 2.6. In [1] Adamy extends the Amick-Schonbek results on the Cauchy problem to the initial value boundary problem posed on \mathbb{R}^+ or a finite interval. She obtains in particular the existence of a weak entropy solution for $x \in \mathbb{R}^+$ with homogeneous or non-homogeneous Dirichlet condition at $x = 0$ and similar results on a bounded interval. She also proves the uniqueness of smooth solutions.

Remark 2.7. Fokas and Pelloni in [23] solved the linearized Amick-Schonbek system on either the half-line or finite interval with suitable boundary conditions, following the unified method of Fokas [22]. The case of the half-line has been revisited in [26].

The long time behavior of the global solutions of the Amick-Schonbek system is unknown, and we present in the section 5 numerical simulations suggesting relevant conjectures.

2.1. The two-dimensional case. The two-dimensional Amick-Schonbek system writes (we have kept the small parameter ϵ):

$$(2.2) \quad \begin{cases} \eta_t + \nabla \cdot \mathbf{v} + \epsilon[\nabla \cdot (\eta \mathbf{v}) = 0 \\ \mathbf{v}_t + \nabla \eta + \epsilon[\frac{1}{2} \nabla |\mathbf{v}|^2 - d \Delta \mathbf{v}_t] = 0. \end{cases}$$

We are not aware of a connection between (2.2) and the two-dimensional Saint-Venant system. The existence on long time $O(1/\epsilon)$ of solutions to the Cauchy problem for (2.2) was established in [36], Theorem 4.4, under the non-cavitation condition $1 + \eta_0 \geq H_0 > 0$ and in [13] without this condition.

Remark 2.8. The long time existence for a two-dimensional Amick-Schonbek system in presence of a non-trivial bathymetry is proven in [32].

3. SOLITARY WAVES OF THE AMICK-SCHONBEK SYSTEM

In this section, we will numerically construct localised traveling wave solutions of the system (1.3), i.e., solutions of the form $\eta = Q(x - Ct)$, $v = V(x - Ct)$ where C is a constant real velocity. We follow the presentation in [14], where the solitary waves were also studied numerically, see also [3]. This ansatz implies for (1.3) after one integration taking care of the vanishing conditions at infinity,

$$(3.1) \quad \begin{aligned} -CQ + V + QV &= 0, \\ -CV + Q + \frac{1}{2}V^2 + cV'' &= 0, \end{aligned}$$

where the prime denotes derivative with respect to the argument. Thus we get

$$(3.2) \quad \begin{aligned} Q &= \frac{V}{C - V}, \\ -CV + \frac{V}{C - V} + \frac{1}{2}V^2 + CV'' &= 0, \end{aligned}$$

Thus solitary waves of the Amick-Schonbek system are given by a single ODE for V , the second equation in (3.2). In order to get solutions that are exponentially decreasing as $e^{-\alpha|x|}$ with $\alpha > 0$ for $|x| \rightarrow \infty$, one must have $\alpha = \sqrt{1 - 1/C^2}$, i.e., $|C| > 1$. Furthermore if V_C is a solution to (3.2), so is $-V_{-C}$, i.e., a change of sign of C implies a change of sign of V . Therefore we will concentrate in the following on the case $C > 1$. Assuming that the function and its derivatives vanish at infinity, the second equation in (3.2) can be integrated once more to give

$$(3.3) \quad \frac{C}{2}((V')^2 - V^2) + \frac{1}{6}V^3 - V - C \ln(1 - V/c) = 0,$$

which implies that V can be given in terms of quadratures. Due to the appearance of the logarithm, it does not seem possible to give V in terms of elementary functions. Note that Q gets very large once the maximum of V is close to C .

It is possible to numerically compute the integral with respect to V , but since we need the solution in the form $V(x)$, this has to be done for all interesting values of x in order to be numerically able to invert the function $x(V)$. Therefore we use here the same approach as in [28]. Since the solitary waves are rapidly decreasing, we can treat them as periodic functions that are smooth on a sufficiently large

torus within the finite numerical precision (we work with double precision where the smallest difference between rational numbers is of the order of 10^{-16}). Thus we consider $x \in L[-\pi, \pi]$ with $L \gg 1$ and use the standard discretisation of the discrete Fourier transform (DFT) $x_n = -\pi L + nh$, $n = 1, 2, \dots, N$ with $h = 2\pi L/N$. The DFT can be conveniently treated with a fast Fourier transform (FFT). We denote the DFT of a discretised function V by \hat{V} . Thus we approximate the second ODE in (3.2)

$$(3.4) \quad F := -\hat{V} + \frac{1}{C(1+k^2)} \left(\frac{1}{2}\widehat{V^2} + \frac{\widehat{V}}{C-V} \right) = 0,$$

which means we have to find the zero of an N -dimensional function, where N is the number of DFT modes. This zero is identified iteratively with a Newton method where the action of the inverse of the Jacobian is computed as in [28] with the Krylov subspace technique GMRES [35].

For concrete computations, we use for $C = 2$, $N = 2^{12}$ DFT modes and $x \in 10[-\pi, \pi]$ with the initial iterate $V^{(0)} = 1.5\text{sech}^2(\alpha x/2)$ where $\alpha = \sqrt{1 - 1/C^2}$. For smaller or larger values of C we apply a continuation technique, i.e., we use the result for $C = 2$ as the initial iterate for slightly larger or smaller values of C . We show the solitary waves for different velocities in Fig. 1. It can be seen that the amplitude of the waves decreases with C , and that the fall-off to infinity becomes slower as expected. It appears that the amplitude of the waves tends to zero for $C \rightarrow 1$.

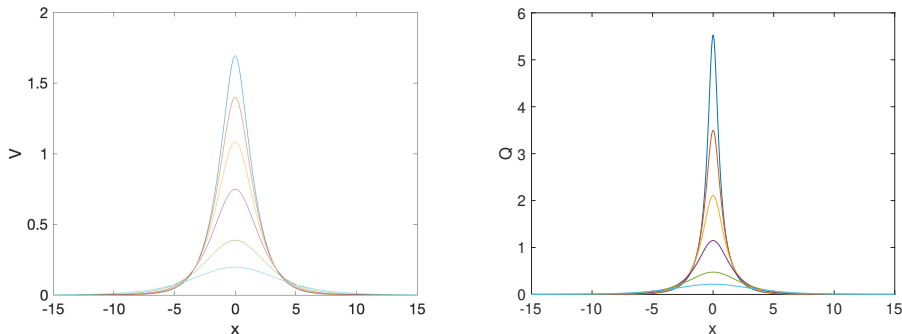


FIGURE 1. Solitary waves of the Amick-Schonbeck system for different values of the velocity $C = 2, 1.8, 1.6, 1.4, 1.2, 1.1$ from top to bottom, on the left V , on the right Q .

For values of C larger than 2, the maximum of V tends closer to C as can be seen in Fig. 2. This implies that the function Q grows strongly. But there is no indication that there is an upper limit for C beyond which there are no solitary waves.

We show in Fig. 3 the L^∞ norm of the functions Q and the related mass (the square of the L^2 norm) for the considered values of C . Both appear to grow algebraically, but it is difficult to access much larger values of C in order to make a numerical conjecture.

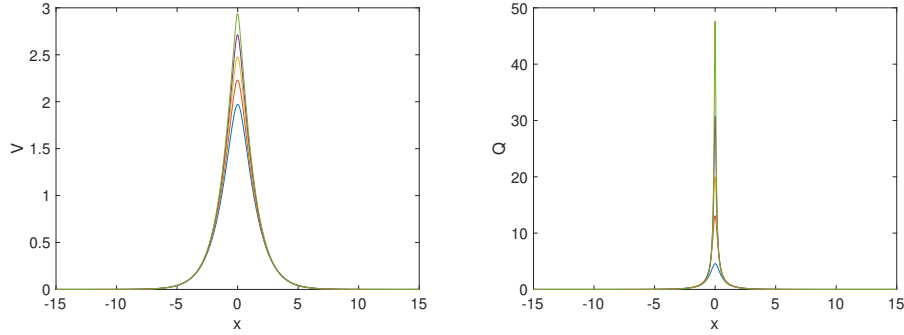


FIGURE 2. Solitary waves of the Amick-Schonbeck system for different values of the velocity $C = 3, 2.8, 2.6, 2.4, 2.2$ from top to bottom, on the left V , on the right Q .

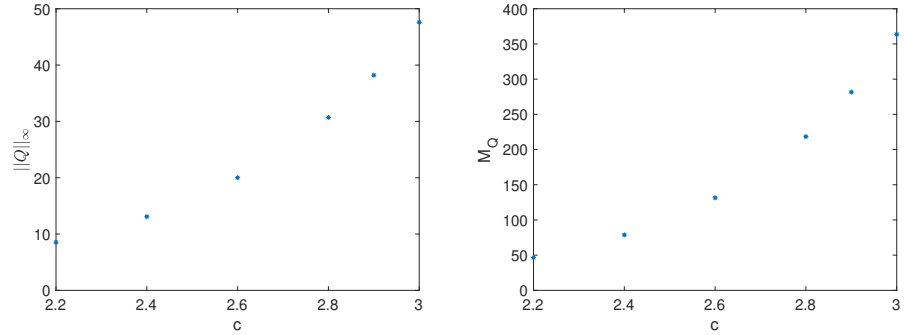


FIGURE 3. The L^∞ norm of the functions Q of Fig. 2.

4. NUMERICAL STUDY OF PERTURBED SOLITARY WAVES

In this section, we numerically study the stability of the solitary waves constructed in the previous section. The results give strong evidence for the first conjecture in the introduction. For the interaction of solitary waves the reader is referred to [14, 3].

For a numerical time evolution of solutions of the Amick-Schonbeck system (1.3), we apply the same DFT discretisation as for the construction of the solitary waves. The time integration is done with the standard explicit 4th order Runge-Kutta method. Since there are apparently no conserved quantities for the system (1.3), which could be used to control the accuracy of the time integration, we test the code at the example of the solitary waves. For the case $C = 2$ in Fig. 1, we use $N_t = 4000$ time steps for $t \leq 1$ and the same spatial resolution as in the previous section. For $t = 1$, the difference between the numerical solution to the system (1.3) for solitary wave initial data and the propagation of the initial data with velocity $C = 2$ is smaller than 10^{-13} on the whole computational domain. Thus the initial data can be propagated with essentially machine precision. Note that this also tests the numerically constructed solitary waves since a non-trivial error there would show up in the time evolution even for arbitrary small time steps.

To consider perturbations of the solitary waves, we use initial data for the system (1.3) which are perturbed solitary waves. We start with initial data of the form

$$(4.1) \quad \eta(x, 0) = \lambda Q(x), \quad v(x, 0) = V(x)$$

where $\lambda \in \mathbb{R}$ with $\lambda \sim 1$. In practice we consider values of λ between 0.9 and 1.1. Note that these are perturbations of the order of 10% and thus by no means small. In a numerical context, one always has to consider perturbations of a certain finite magnitude in order to see effects of the perturbation on the solution in finite time. We use $N_t = 10^4$ time steps for $t \leq 10$ for $\lambda = 1.1$. The solution at the final time is shown in Fig. 4. It can be seen that radiation is propagating to the left as a consequence of the perturbation, but that the initial hump is essentially unchanged.

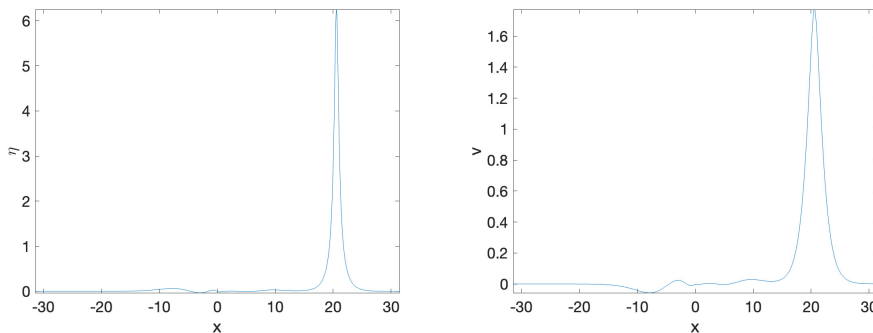


FIGURE 4. Solution to the Amick-Schonbeck system (1.3) for the initial data $\eta(x, 0) = 1.1Q_2(x)$, $v(x, 0) = V_2(x)$ for $t = 10$, on the left η , on the right v .

The interpretation of the humps as a solitary wave of slightly larger velocity (due to the large perturbation, the final state will be a slightly different solitary wave) is confirmed by the L^∞ norms of η and v in Fig. 5. Both norms appear to reach asymptotically a constant value at a slightly higher level than for the unperturbed solitary wave. Note that the solitary waves do not show a simple scaling in C . Thus it is not obvious with which velocity the final state in Fig. 5 propagates. The small oscillations in the L^∞ norm are due to the norm being evaluated on the numerical grid whilst the maximum does not have to be located on a grid point, and that radiation can reenter the computational domain on the other side since we work on a torus.

The results are similar for initial data of the form (4.1) with $\lambda = 0.9$. The solutions for $t = 10$ can be seen in the upper row of Fig. 6. Once more they appear to be solitary waves plus radiation, but this time with slightly smaller velocity than the unperturbed solitary wave. This interpretation is confirmed by the L^∞ norms shown in the lower row of the same figure.

Thus the solitary waves for $C = 2$ appear to be stable for the considered perturbation. In order to show that this result does not depend on a specific perturbation, we study also perturbations of the form

$$(4.2) \quad \eta(x, 0) = Q_c(x) \pm \mu \exp(-x^2), \quad v(x, 0) = V_c(x),$$

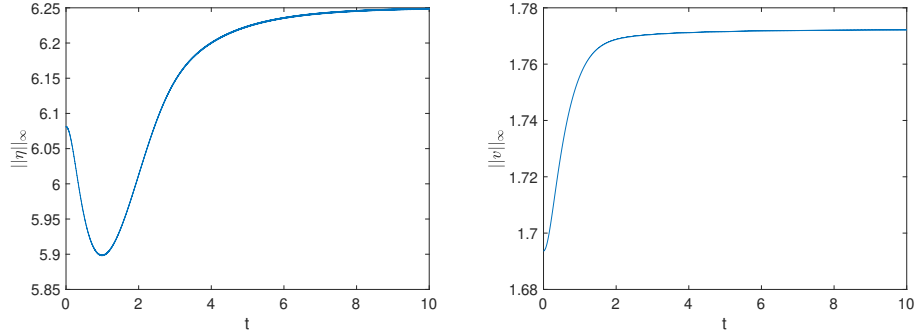


FIGURE 5. L^∞ norms of the solution to the Amick-Schonbeck system (1.3) for the initial data $\eta(x, 0) = 1.1Q_2(x)$, $v(x, 0) = V_2(x)$ in dependence of time, on the left for η , on the right for v .

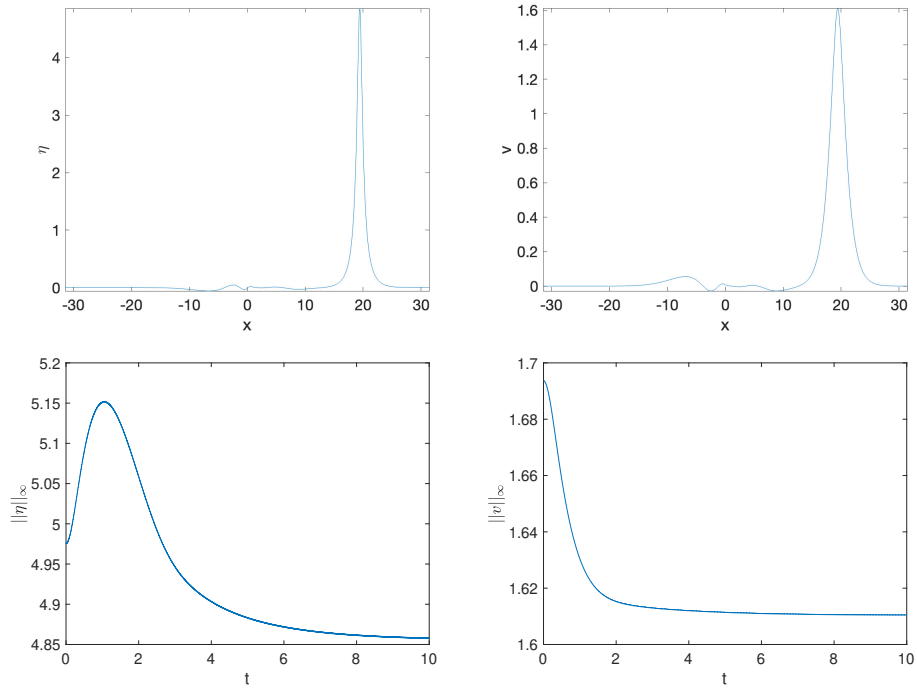


FIGURE 6. Solution to the Amick-Schonbeck system (1.3) for the initial data $\eta(x, 0) = 0.9Q_2(x)$, $v(x, 0) = V_2(x)$ for $t = 10$, on the left η , on the right v , in the upper row the solutions for $t = 10$, in the lower row the respective L^∞ norms in dependence of time.

i.e., we add or subtract a small Gaussian to the solitary wave. Once more the solution at the final time appears to be a solitary wave of slightly larger (for the + sign) or smaller (for the - sign) velocity.

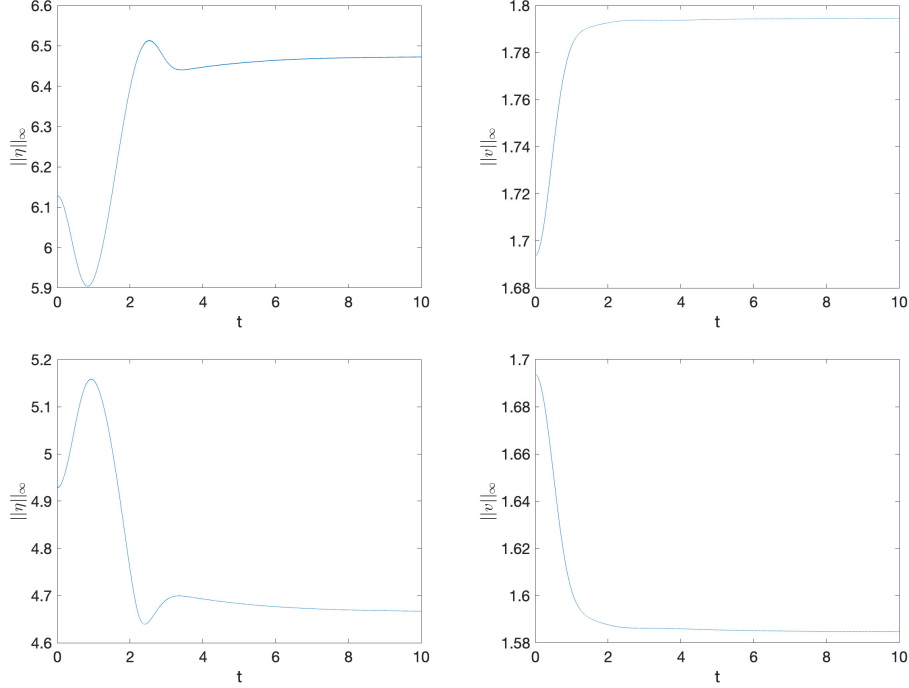


FIGURE 7. L^∞ norms of the solution to the Amick-Schonbeck system (1.3) for the initial data $\eta(x, 0) = Q_c(x) \pm 0.6 \exp(-x^2)$, $v(x, 0) = V_2(x)$, on the left η , on the right v , in the upper row for the + sign, in the lower row for the - sign.

The situation is somewhat different if a solitary wave with a velocity close to 1 is considered. Here smaller perturbations have to be applied, and it will take much longer times to get close to a final state. Therefore we consider the same perturbations as above with smaller values for λ , μ for the solitary wave with $C = 1.1$ on a larger torus $x \in 40[-\pi, \pi]$. We use $N = 2^{14}$ DFT modes and $N_t = 2 * 10^4$ time steps for $t \leq 100$. In Fig. 8 we show the L^∞ norms of the solutions to the Amick-Schonbeck system (1.3) for initial data of the form (4.1) for $\lambda = 1.01$ and $\lambda = 0.99$, i.e., perturbations of the order of 1%. It can be seen that the L^∞ norms only reach final states very slowly, but it appears that the latter are again a solitary wave plus radiation.

We also consider initial data of the form (4.2) for solitary waves with velocity $C = 1.1$, but again a perturbation of the order of 1%, $\mu = 0.002$. The L^∞ norms of the solutions can be seen in Fig. 9.

The situation for values of C larger than 2 is similar to the one for $c \sim 1$. We use $N = 2^{15}$ DFT modes for $x \in 20[-\pi, \pi]$ and $N_t = 10^5$ time steps for $t \leq 10$. A small perturbation of the form (4.1) as in Fig. 8 leads for $C = 3$ to a small perturbation in the L^∞ norm of v indicating the final state is a solitary wave with a slightly higher velocity. But as can be seen in Fig. 10 this implies a strong change of the L^∞ norm of η since the latter varies rapidly with C for larger values of C , see Fig. 2. latter is strongly growing

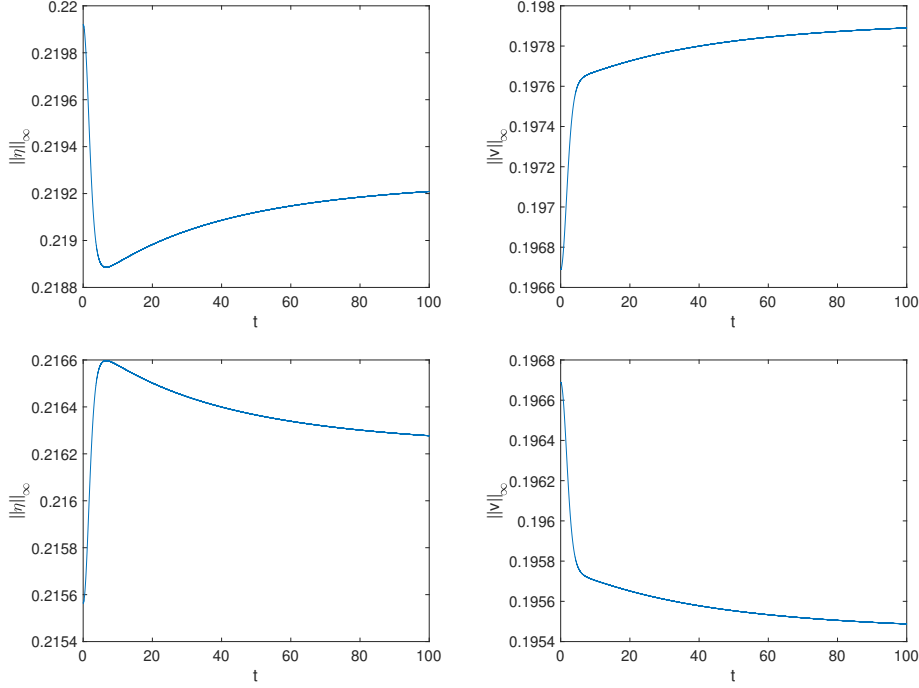


FIGURE 8. L^∞ -norms of the solution to the Amick-Schonbeck system (1.3) for initial data of the form (4.1) with $C = 1.1$, on the left η , on the right v , in the upper row for the $\lambda = 1.01$, in the lower row for the $\lambda = 0.99$.

5. LOCALISED INITIAL DATA

In this section we discuss the time evolution of localised initial data for the Amick-Schonbeck system (1.3). We consider initial data of the form

$$(5.1) \quad \eta(x, 0) = A \exp(-x^2), \quad v(x, 0) = 0,$$

where A is a positive constant. The results give strong evidence to the soliton resolution conjecture for this system.

We first consider the case of a large constant, $A = 10$. We use $N = 2^{14}$ DFT modes for $x \in 10[-\pi, \pi]$ and $N_t = 10^4$ time steps for $t \leq 10$. For symmetry reasons the initial hump in η splits into two humps traveling towards positive and negative values of x respectively. This can be seen in Fig. 11 on the left. The function v is positive for positive values of x and negative for negative x .

The final state of the solution appears to be two solitary waves, one with positive velocity, and one with negative velocity. This interpretation is confirmed by the L^∞ norms of the solution in Fig. 12. As expected from the stability of the solitary waves studied in the previous section, solitary waves seem to appear in the long time behavior of the solutions in accordance with the soliton resolution conjecture.

For smaller values of A , say $A = 1$, the same phenomenon as in the previous section is observed, that much larger times are needed to observe the formation of

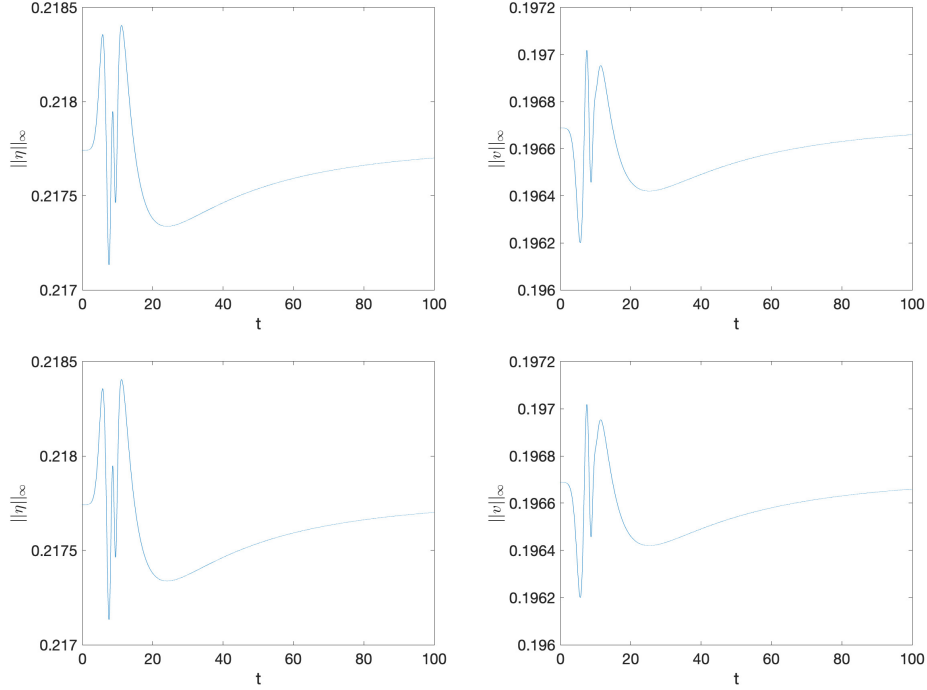


FIGURE 9. L^∞ norms of the solution to the Amick-Schonbeck system (1.3) for the initial data $\eta(x, 0) = Q_C(x) \pm 0.002 \exp(-x^2)$, $v(x, 0) = V_C(x)$ with $C = 1.1$, on the left η , on the right v , in the upper row for the $+$ sign, in the lower row for the $-$ sign.

solitary waves with $C \sim 1$. We use the same number of DFT modes, but on a larger torus, $x \in 40[-\pi, \pi]$ and $N_t = 2 * 10^4$ time steps for $t \leq 50$. The solution at the final time is shown in Fig. 13. There are again two humps, but now with strong radiation in comparison to the amplitude of the presumed solitary waves.

The L^∞ norms of these solutions can be seen in Fig. 14. They appear to saturate, but the final state, which seems to be solitary waves plus radiation, is obviously not yet reached.

6. NON-CAVITATION INITIAL DATA

In this section we study the Amick-Schonbeck system (1.3) for initial data that violate the non-cavitation condition $1 + \eta > 0$ or that are close to violating it. The results are similar to what was found in [20] for the Serre-Green-Naghdi equation and give strong evidence for the second conjecture in the introduction.

As we will show below, it is numerically challenging to study the solution of the system (1.3) for initial data that are close to or actually violating the non-cavitation condition $1 + \eta > 0$ since the solution appears to become singular or almost singular in finite time. We consider initial data of the form

$$(6.1) \quad \eta(x, 0) = -\kappa \exp(-x^2), \quad v(x, 0) = 0,$$

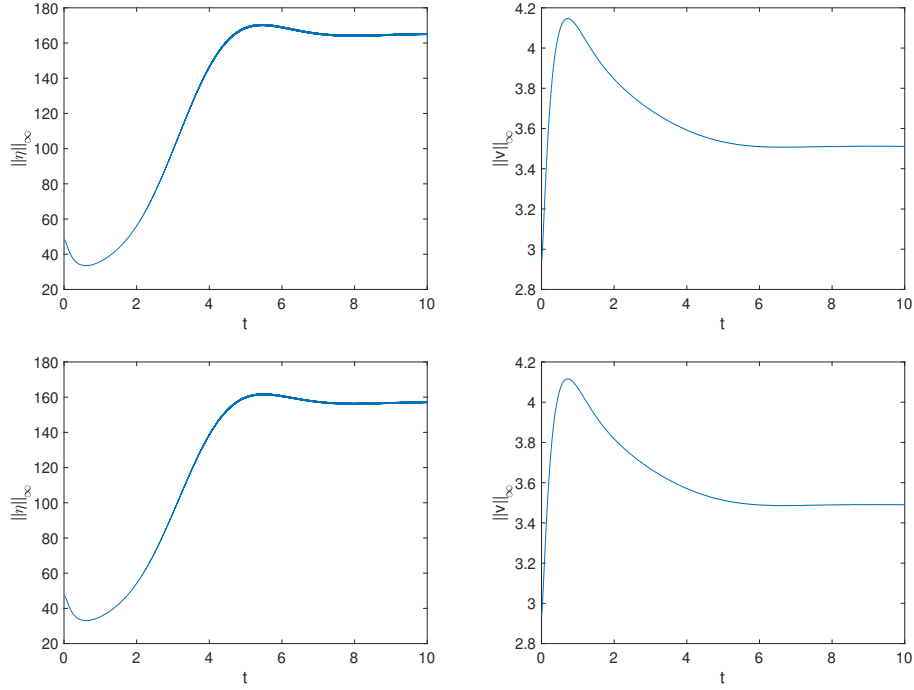


FIGURE 10. L^∞ -norms of the solution to the Amick-Schonbeck system (1.3) for initial data of the form (4.1) with $C = 3$, on the left η , on the right v , in the upper row for the $\lambda = 1.01$, in the lower row for the $\lambda = 0.99$.

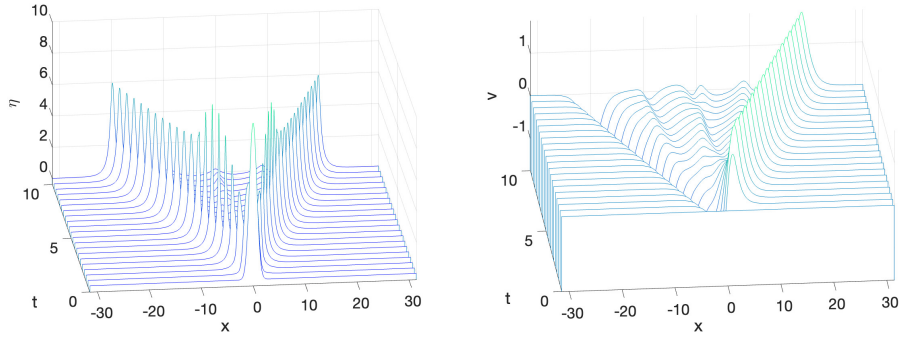


FIGURE 11. Solution to the Amick-Schonbeck system (1.3) for initial data of the form (5.1) with $A = 10$, on the left η , on the right v .

where κ is a positive constant. First we consider the case $\kappa = 1$, i.e., an example violating the non-cavitation condition in one point, $x = 0$ for $t = 0$. We use $N = 2^{18}$ DFT modes for $x \in 3[-\pi, \pi]$ and $N_t = 10^5$ time steps for $t \leq 5$, close to the accessible accuracy with double precision arithmetics. It can be seen that the initial depression in η disappears and that it eventually develops a strongly peaked

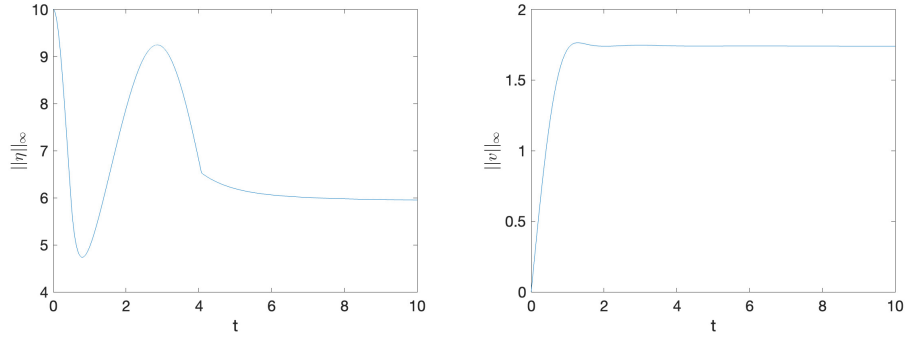


FIGURE 12. L^∞ norms of the solution to the Amick-Schonbeck system (1.3) for initial data of the form (5.1) with $A = 10$, on the left η , on the right v .

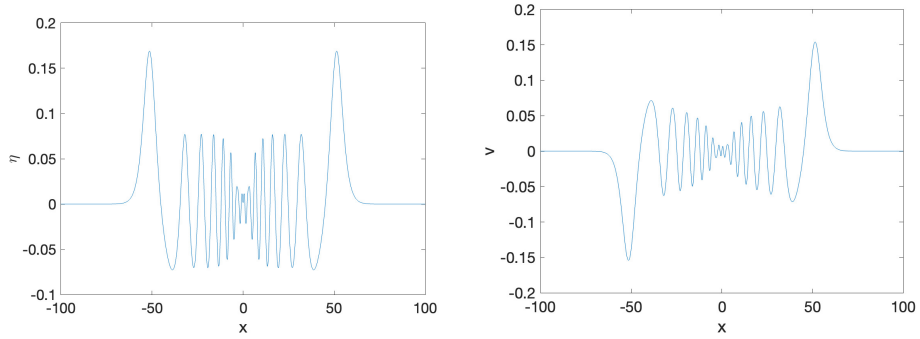


FIGURE 13. Solution to the Amick-Schonbeck system (1.3) for initial data of the form (5.1) with $A = 1$ for $t = 50$, on the left η , on the right v .

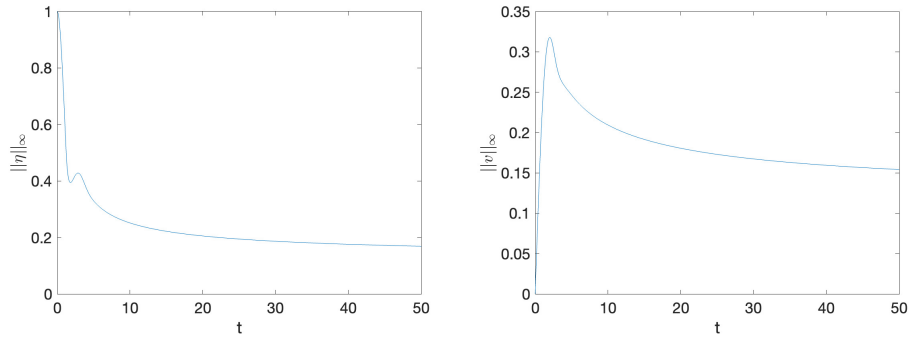


FIGURE 14. L^∞ norms of the solution to the Amick-Schonbeck system (1.3) for initial data of the form (5.1) with $A = 1$, on the left η , on the right v .

maximum at a high elevation. The function v on the other hand is as before odd in x with a maximum to the left and a minimum to the right of the origin. For larger times, a new small oscillation of this function appears near the origin.

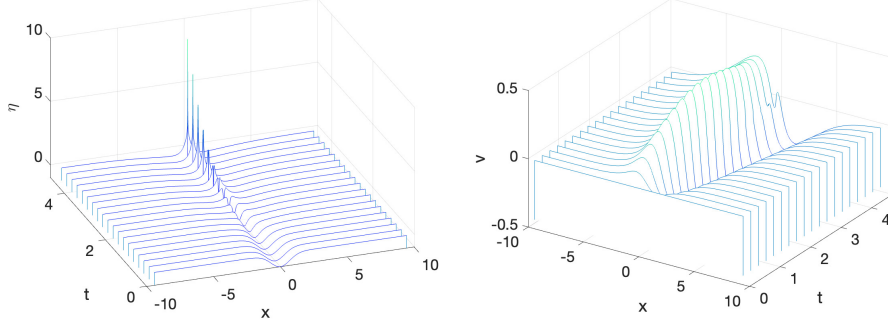


FIGURE 15. Solution to the Amick-Schonbeck system (1.3) for initial data of the form (6.1) with $\kappa = 1$, on the left η , on the right v .

We show the solution at the last recorded time $t \sim 4.68$ in Fig. 16. It can be seen that the function η at this time is strongly peaked near the origin, and that v has a strong gradient there.

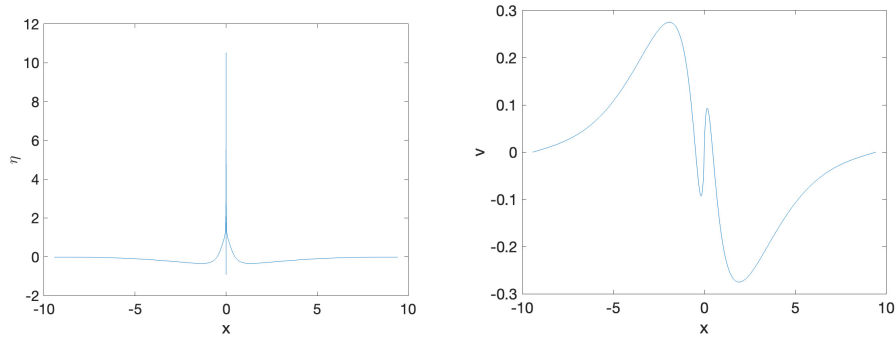


FIGURE 16. Solution to the Amick-Schonbeck system (1.3) for initial data of the form (6.1) with $\kappa = 1$ for $t \sim 4.68$, on the left η , on the right v .

A close-up of the the function η near the origin, see Fig. 17, reveals that there is a strong cusp-like gap near the origin. It is this cusp-like structure that is numerically difficult to resolve and potentially singular, not the peak. Note that the function η appears to be negative at the minimum in the close-up, but just at this point. The L^∞ norm of the function η on the right of the same figure shows that the peak near the origin is growing which could correspond to an L^∞ blow-up.

An interesting approach to numerically study singularities in a Fourier spectral method was introduced by Sulem, Sulem and Frisch in [38]. It is well known that an essential singularity in the complex plane of the form $u \sim (z - z_j)^{\mu_j}$, $\mu_j \notin \mathbb{Z}$, with $z_j = \alpha_j - i\delta_j$ in the lower half plane ($\delta_j \geq 0$) implies for $k \rightarrow \infty$ the following

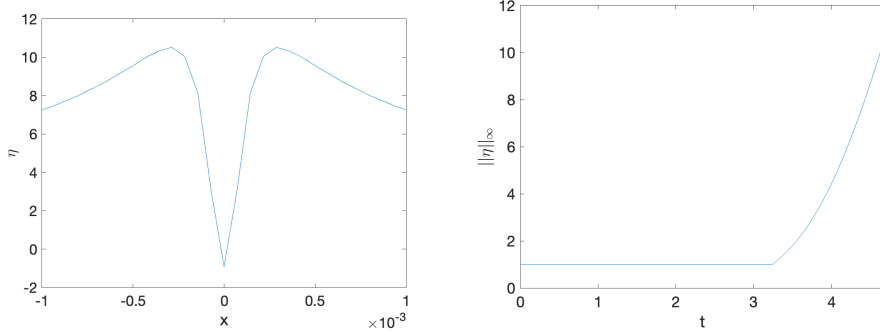


FIGURE 17. Close-up of the function η on the left of Fig. 16 on the left and the L^∞ norm of η in dependence of time on the right.

asymptotic behavior of the Fourier transform (see e.g. [15], here denoted in the same way as the DFT),

$$(6.2) \quad \hat{u}(k) \sim \sqrt{2\pi} \mu_j^{\mu_j + \frac{1}{2}} e^{-\mu_j} \frac{(-i)^{\mu_j + 1}}{k^{\mu_j + 1}} e^{-ik\alpha_j - k\delta_j}.$$

For a single such singularity with positive δ_j , the modulus of the Fourier transform decreases exponentially for large k until $\delta_j = 0$, when this modulus has an algebraic dependence on k for large $|k|$. This behavior can also be seen in the discrete version of the Fourier transform, the DFT. For the example in Fig. 16, the DFT coefficients are shown in Fig. 18. The algebraic decay of the DFT coefficients for large $|k|$ indicates that a singularity of the approximated function in the complex plane hits the real axis in this case. The DFT coefficients are fitted as discussed in [27], $\ln |\hat{\eta}|$ with linear regression to $\mu \ln |k| - \delta |k| + \text{const}$. Concretely two values of k are chosen, $k_{min} \gg 1$ and $k_{max} < N/2/L$ such that the following results do not change considerably if these values are slightly modified (in other words, an asymptotic region is identified with $k \gg 1$ but a cutoff before reaching the level of rounding errors). A standard regression analysis of the relation (6.2) leads to the matrix

$$\mathcal{M} = \sum_{k=k_{min}}^{k_{max}} \begin{pmatrix} (\ln k)^2 & k \ln k & \ln k \\ k \ln k & k^2 & k \\ \ln k & k & 1 \end{pmatrix}$$

and $\alpha = \mathcal{M}^{-1} \mathbf{v}$, where

$$\mathbf{v} = \sum_{k=k_{min}}^{k_{max}} \begin{pmatrix} (\ln(k)) \hat{u}(k) \\ k \hat{u}(k) \\ \hat{u}(k) \end{pmatrix}$$

and where the vector α has the components $\begin{pmatrix} \mu + 1 \\ \delta \\ \text{const} \end{pmatrix}$. The code is stopped when δ is

smaller than the smallest distance on the numerical grid since smaller values cannot be numerically distinguished from zero in this case. In the considered example this happens for $t \sim 4.6809$. We get for the critical exponent of \hat{v} the value 0.37 and for the one for $\hat{\eta}$ the value -0.85 . Note that the fitting of these critical exponents comes with a non negligible uncertainty, see the discussion in [27], since it corresponds to fitting a logarithmic correction of a linear dependence in k where the latter is

close to vanishing. The data is compatible with $1/3$ for v , a cubic cusp as in the generic break-up of solutions to the Hopf equation, and with -1 for η , a simple pole. However, the behavior of the DFT coefficients clearly indicates that there is an L^∞ blow-up in η whereas a cusp forms in v .

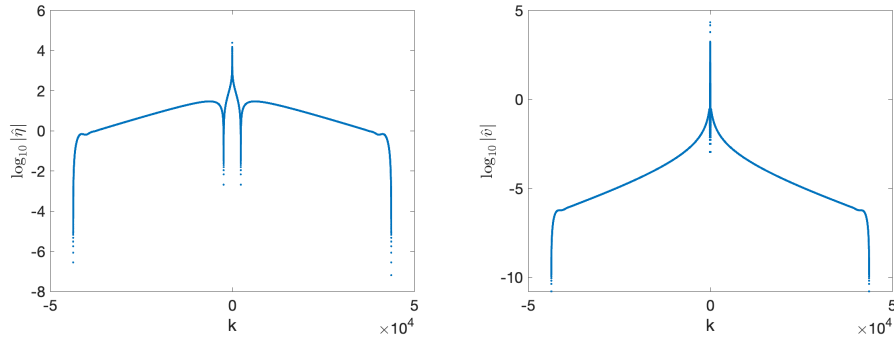


FIGURE 18. Fourier coefficients of the solution to the Amick-Schonbeck system (1.3) for initial data of the form (6.1) with $\kappa = 1$ for $t \sim 4.68$, on the left η , on the right v .

For initial data which come close to violating the non-cavitation condition, for instance (6.1) with $\kappa = 0.9$, the solution shows qualitatively the same behavior as can be seen in Fig. 19. But there is no indication of the formation of a singularity in this case.

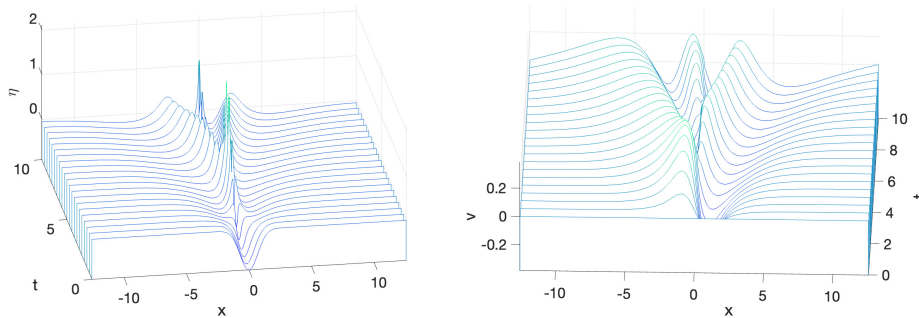


FIGURE 19. Solution to the Amick-Schonbeck system (1.3) for initial data of the form (6.1) with $\kappa = 0.9$, on the left η , on the right v .

The DFT coefficients show exponential decrease during the whole computation. The solution for $t = 10$ in Fig 20 shows no indication of the formation of a singularity both in v and in a close-up of η . The L^∞ norms of both functions decrease with time for large t .

7. DISPERSIVE SHOCK WAVES

In this section we study the possible formation of zones of rapid modulated oscillations called dispersive shock waves (DSWs).

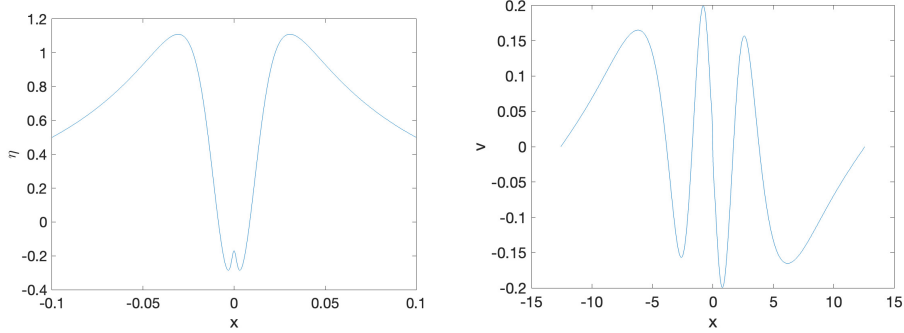


FIGURE 20. Solution to the Amick-Schonbeck system (1.3) for initial data of the form (6.1) with $\kappa = 0.9$ for $t = 10$, on the left a close-up of η , on the right v .

A convenient way to study the appearance of DSWs in nonlinear dispersive PDEs is to consider data with support of length scales of order $1/\varepsilon$, $\varepsilon \gg 1$, on time scales of order $1/\varepsilon$. This can be achieved by rescaling time and space by a factor of ε , which leads for the system (1.3) to a system containing a small parameter (we keep the same notation as in (1.3) for simplicity)

$$(7.1) \quad \begin{cases} \eta_t + v_x + (\eta v)_x = 0 \\ v_t + \eta_x + vv_x - \varepsilon^2 v_{xxt} = 0. \end{cases}$$

The formal limit $\varepsilon \rightarrow 0$ leads to the Saint-Venant system

$$(7.2) \quad \begin{cases} \eta_t + v_x + (\eta v)_x = 0 \\ v_t + \eta_x + vv_x = 0, \end{cases}$$

expected to develop shocks for general initial data in finite time.

We do not study this aspect here, but the dispersive regularisation of these shocks via (7.1). We consider the initial data $\eta(x, 0) = \exp(-x^2)$, $v(x, 0) = 0$ as before for several values of ε with $N = 2^{14}$ DFT modes for $x \in 3[-\pi, \pi]$ and $N_t = 10^4$ time steps for $t \leq 5$. In Fig. 21 we show the solution for $\varepsilon = 0.1$ in dependence of time. It can be seen that as before the function η remains symmetric, and that two humps form. There is a steepening of the gradients near these humps which would form shocks in the Saint Venant system (7.2), but which will lead to the formation of oscillations in the dispersive system (7.1) near the location of the shocks of the Saint-Venant system. The function v shows a similar behavior, but is odd. Note that the humps in the DSWs can be interpreted as solitary waves that look slightly different than before since both x and t have been rescaled.

A close-up of the oscillatory zone for the solutions at the final time in Fig. 21 is shown in Fig. 22 supporting the soliton resolution conjecture.

We show the solution for $t = 5$ for several values of ε in Fig. 23 in a close-up of the oscillatory zone for positive x . It can be seen that the oscillations become more and more rapid for smaller ε , and that they are also more and more confined to a well defined zone sometimes referred to as Whitham zone. This behavior is reminiscent of the well studied case of the KdV equation, see for instance [29].

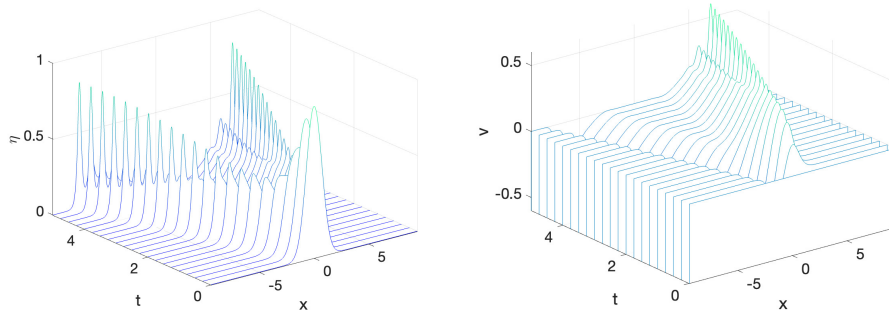


FIGURE 21. Solution to the Amick-Schonbeck system (7.1) for $\varepsilon = 0.1$ and initial data $\eta(x, 0) = \exp(-x^2)$, $v(x, 0) = 0$, on the left η , on the right v .

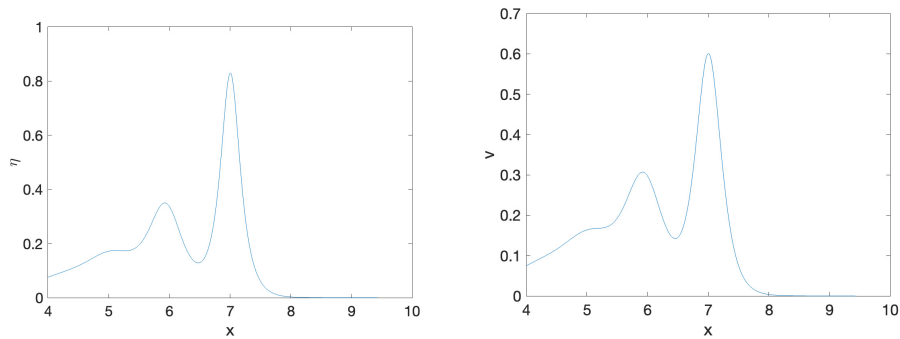


FIGURE 22. Close-up of the solutions to the Amick-Schonbeck system (7.1) for $\varepsilon = 0.1$ and initial data $\eta(x, 0) = \exp(-x^2)$, $v(x, 0) = 0$ for $t = 5$, on the left η , on the right v .

8. CONCLUSION

In this paper we have numerically studied certain aspects of solutions to the Amick-Schonbeck system (1.3). The focus was on the asymptotic stability of the solitary waves for a wide range of the velocities C , and their appearance in the long time behavior of initial data from the Schwartz class. We have also addressed the appearance of DSWs that seem to be similar to DSWs in KdV solutions. In addition we have established the appearance of a blow-up in solutions for initial data not satisfying the non-cavitation condition.

It is an interesting question whether similar results can be obtained in two spatial dimensions. In [21] it was found that the 2D Serre-Green-Naghdi equations show a defocusing effect similar to the Kadomtsev-Petviashvili II equation, see [29]. No solitary waves localised in 2D were found. The question is whether there are such solutions for the 2D Amick-Schonbeck system (2.2). If they exist, their stability has to be studied as well as the long time behavior of solutions for localised initial data. The possibility of a blow-up in 2D has to be explored. This will be the topic of future work.

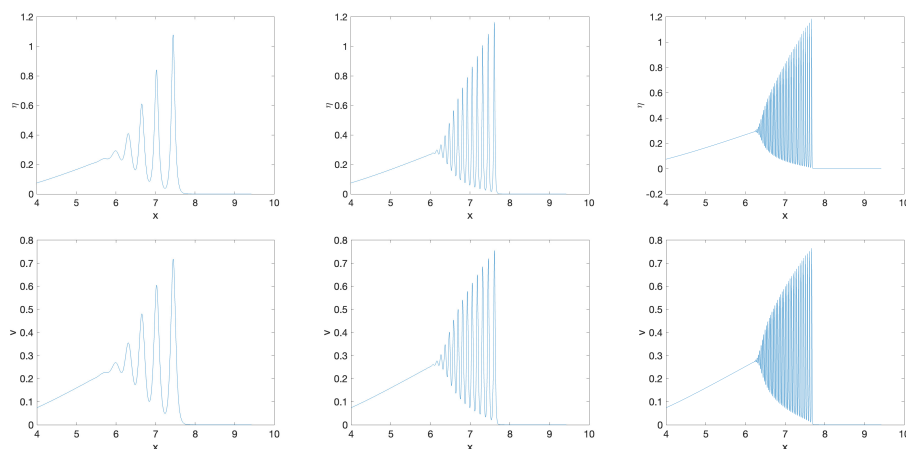


FIGURE 23. Close-up of the solutions to the Amick-Schonbeck system (7.1) for $\varepsilon = 10^{-1.5}, 10^{-2}, 10^{-2.5}$ (from left to right) and initial data $\eta(x, 0) = \exp(-x^2)$, $v(x, 0) = 0$ for $t = 5$, upper row η , lower row v .

Acknowledgements. CK was partially supported by the ANR-17-EURE-0002 EIPHI and by the European Union Horizon 2020 research and innovation program under the Marie Skłodowska-Curie RISE 2017 grant agreement no. 778010 IPaDEGAN.

REFERENCES

1. K. ADAMY, *Existence of solutions for a Boussinesq system on the half line and on a finite interval*, Discrete Cont. Dyn. Systems **29** (1) (2011), 25-49.
2. C.J. AMICK, *Regularity and uniqueness of solutions for the Boussinesq system of equations*, J. Differential Eq. **54** (1) (1984), 231-247.
3. D. ANTONOPOULOS AND V. DOUGALIS, *Numerical solution of the "classical" Boussinesq system*, Math. Comp. Simul. **82** (2012), 984-1007.
4. D. ANTONOPOULOS AND V. DOUGALIS, *Error estimates for Galerkin approximations of the "classical" Boussinesq system*, Math. Comp. **82** (2013), no. 282, 689-717.
5. D.C. ANTONOPOULOS, V. A. DOUGALIS AND D. E. MITISOTAKIS, *Galerkin approximations of periodic solutions of Boussinesq systems*, Bull. Greek Math. Soc. **57** (2010), 13-30.
6. H. BERESTYCKI AND P.-L. LIONS, *Nonlinear scalar field equation I*, Arch. Rat. Mech. Anal. **32** (1983), 313-346.
7. L. BRUDVIK-LINDNER, D. MITSOTAKIS AND A. E. TZAVARAS, *Oscillatory and regularized shock waves for a dissipative Peregrine-Boussinesq system*, IMA Journal of Applied Mathematics (2023) <https://doi.org/10.1093/imamat/hxad030>
8. J. L. BONA, T. COLIN AND D. LANNES, *Long-wave approximation for water waves*, Arch. Ration. Mech. Anal. **178**, (2005), 373-410.
9. J. L. BONA, M. CHEN AND J.-C. SAUT, *Boussinesq equations and other systems for small-amplitude long waves in nonlinear dispersive media I : Derivation and the linear theory*, J. Nonlinear Sci. **12** (2002), 283-318.
10. J. L. BONA, M. CHEN AND J.-C. SAUT, *Boussinesq equations and other systems for small-amplitude long waves in nonlinear dispersive media. II : The nonlinear theory*, Nonlinearity **17** (2004) 925-952.
11. J. BOUSSINESQ, *Théorie des ondes et des remous qui se propagent le long d'un canal rectangulaire horizontal, en communiquant au liquide contenu dans ce canal des vitesses sensiblement pareilles de la surface au fond*, J. Math. Pures Appl. **7** (2) (1872), 55-108.

12. L.F.J. BROER, *Approximate equations for long water waves*, Appl. Sci. Res. **31** (1975), 377-395.
13. C. BURTEA, *New long time existence results for a class of Boussinesq-type systems*, J. Math. Pures Appl. **106** (2) (2016), 203-236.
14. MIN CHEN, *Solitary-wave and multi-pulsed traveling-wave solutions of Boussinesq systems*, Appl. Anal. **75** (1-2) (2000), 213-240.
15. G. CARRIER AND M. K. C. PEARSON, *Functions of a Complex Variable, Theory and Technique*, Society for Industrial and Applied Mathematics (SIAM), Philadelphia, PA, 2005.
16. O. DARRIGOL, *Worlds of flow. A hydrodynamics from the Bernoullis to Prandtl*, Oxford University Press 2005.
17. O. DARRIGOL, *The Spirited Horse, the Engineer, and the Mathematician : Water Waves in Nineteenth -Century Hydrodynamics*, Arch. Hist. Exact Sci. **58** (2003), 21-95.
18. O. DARRIGOL, *Joseph Boussinesq's legacy in fluid mechanics*, C.R. mechanics **345** (2017), 427-445.
19. M.W. DINGEMANS, *Water wave propagation over uneven bottoms. Part 2- Non-linear Wave Propagation*, Advances Series on Ocean Engineering-Volume 13. World Scientific, (2000).
20. V. Duchêne, C. Klein, *Numerical study of the Serre-Green-Naghdi equations and a fully dispersive counterpart*, Discr. & Cont. Dyn. Syst. B, **27**(10), 5905-593 (2021) doi: 10.3934/dcdsb.2021300
21. S. Gavriluk, C. Klein, *Numerical study of the Serre-Green-Naghdi equations in 2D*, <http://arxiv.org/abs/2306.09731>
22. A.S. FOKAS, *A unified transform method for solving linear and certain nonlinear PDE's*, Proc. Roy. Soc. A **453** (1997), 1411-1443.
23. A.S. FOKAS AND B. PELLONI, *Boundary value problems for Boussinesq type systems*, Analysis and Geometry **8** (2005), 59-96.
24. G. KOUNADIS, D.C. ANTONOPOULOS, V.A. DOUGALIS, *Galerkin finite element methods for the numerical solution of two classical Boussinesq type systems over variable bottom*, Wave Motion **102** (2021), 102715.
25. M.D. GROVES, *Hamiltonian long-wave approximations for water waves in a uniform channel*, in Nonlinear Dispersive Wave Systems, Lokenath Debnath Ed. World Scientific (1992), 99-125.
26. C.M. JOHNSTON, C.T. GARTMAN AND D. MANTZAVINOS, *The linearized classical Boussinesq system on the half-line*, Studies in Applied Math. **146** (2021), 635-657
27. C. KLEIN AND K. ROIDOT, *Numerical study of shock formation in the dispersionless Kadomtsev-Petviashvili equation and dispersive regularizations*, Physica D, Vol. 265, 1–25, 10.1016/j.physd.2013.09.005 (2013).
28. C. KLEIN AND J.-C. SAUT, *A numerical approach to blow-up issues for dispersive perturbations of Burgers' equation*, Physica D: Nonlinear Phenomena (2015), 46-65, 10.1016/j.physd.2014.12.004
29. C. KLEIN AND J.-C. SAUT, *Nonlinear dispersive equations — Inverse Scattering and PDE methods*, Applied Mathematical Sciences 209 (Springer, 2022)
30. D. LANNES, *Water waves : mathematical theory and asymptotics*, Mathematical Surveys and Monographs, vol 188 (2013), AMS, Providence.
31. B. MELINAND, *Dispersion estimates for non-homogeneous radial phases : an application to weakly dispersive equations and water waves models*, J. Funct. Analysis (2023).
32. B. MESOGNON-GIREAU, *The Cauchy problem on large time for a Boussinesq-Peregrine equation with large topography variations*, Ann. I.H. Poincaré-AN **34** (2017), 89-118.
33. L. MOLINET, R. TALHOUK AND I. ZAITER, *The classical Boussinesq system revisited*, Nonlinearity **34** (2) (2021), 744-775.
34. D.H. PEREGRINE, *Long waves on a beach*, J. Fluid Mech. **27** (1967), 815-827.
35. Y. SAAD, M. SCHULTZ, *GMRES: A generalized minimal residual algorithm for solving non-symmetric linear systems*, SIAM J. Sci. Stat. Comput. **7** (3), 856–869 (1986).
36. J. C. SAUT, C. WANG AND L. XU, *The Cauchy problem on large time for surface waves Boussinesq systems II*, SIAM Journal on Mathematical Analysis, **49** (4) (2017), 2321–2386.
37. M.E. SCHONBEK, *Existence of solutions to the Boussinesq system of equations*, J. Differential Eq. **42** (1981), 325-352.
38. C. SULEM, P. SULEM, AND H. FRISCH, *Tracing complex singularities with spectral methods*, J. Comp. Phys., **50** (1983), pp. 138–161.

39. M. H. TENG AND T. Y. WU, *Nonlinear water waves in channels of arbitrary shape*, J. Fluid Mech. **242** (1992), 211-233.
40. T. Y. WU, *A bidirectional long wave model*, Methods and Applications of Analysis. **1** (1) (1994), 108-117.

INSTITUT DE MATHÉMATIQUES DE BOURGOGNE, UMR 5584, INSTITUT UNIVERSITAIRE DE FRANCE,
UNIVERSITÉ DE BOURGOGNE-FRANCHE-COMTÉ, 9 AVENUE ALAIN SAVARY, 21078 DIJON CEDEX,
FRANCE

Email address: `Christian.Klein@u-bourgogne.fr`

LABORATOIRE DE MATHÉMATIQUES, UMR 8628,, UNIVERSITÉ PARIS-SACLAY ET CNRS, 91405
ORSAY, FRANCE

Email address: `jean-claude.saut@universite-paris-saclay.fr`